PERGAMON

Building and Environment 34 (1999) 129–138

BUILDING AND ENVIRONMENT

Comparison between computed and field measured thermal parameters in an atrium building

Abdelaziz Laouadi, Morad R. Atif*

Indoor Environment Research Program, Institute for Research in Construction, National Research Council Canada, Montreal Road, Ottawa, Ontario, Canada, K1A 0R6

Received 15 July 1997; revised 2 September 1997; accepted 19 January 1998

Abstract

This paper presents a comparison study between simulation and filed measurements of thermal parameters of an atrium building in Ottawa, Canada. The selected atrium was an enclosed three-storey building with a pyramidal skylight. The atrium was fully conditioned and has open corridors at each storey connecting it to adjacent spaces. The atrium space was used for circulation and reception while adjacent spaces are offices and meeting rooms. The atrium was monitored in June 1995 and in December 1995 to consider extreme conditions of the outdoor climate. The simulation results were obtained using ESP-r computer program. The comparison included those of predicted and measured solar radiation entering the atrium space at the rooftop, and predicted and measured indoor temperatures of the atrium floors. Results for the solar radiation showed good agreement between the measured and predicted values. When the mechanical system was turned off, the predicted temperatures were within ± 2°C of the measured temperatures in winter. In summer, however, the predicted temperatures were 2–3°C higher than the measured temperatures.

Keywords: Atrium; Field measurements; Simulation; Comparison

1. Introduction

Energy simulation software packages for conventional office buildings usually do not apply to atrium buildings. This is because atria involve more complex and significant thermal phenomena, which are absent or less significant in room buildings. The large size of the atrium space results in temperature stratification and three-dimensional buoyancy-driven flow resulting from solar heat gains, and perhaps, from internal heat gains. Furthermore, the large atrium fenestration includes more complex shapes (dome, pyramid, cylinder) than the planar shape usually seen in conventional room buildings. As a result, the prediction of the incoming solar radiation becomes a very difficult task. In addition, solar radiation entering the atrium space through fenestration experiences multiple reflections and transmissions to adjacent spaces.

Prediction of energy consumption and thermal performance of atria have usually been conducted using existing energy simulation programs developed for conventional office buildings [1–3]. The rationale has usually been to adapt existing programs to atria. Computational fluid dynamic (CFD) programs have also been used to study temperature stratification and air flow patterns inside atrium spaces [4, 5]. In spite of being powerful tools for predicting indoor patterns, applying CFD programs to atria could be tedious and not practical due to the dynamic behaviour of the building, which often results in excessive calculation time. Furthermore, CFD simulation programs have yet to be validated in atrium spaces. A trade-off between applying office building energy programs and full CFD programs should be sought by enhancing office building energy computer programs to deal effectively with the thermal behaviour in atrium spaces. Validation studies for atria, similar to that of conventional office buildings [6–9], should be conducted. This is very important in establishing energy guidelines for atria, which are proliferating with an increasing frequency all over the world due to their daylighting and aesthetic features [10, 11]. Because of numerous claims of high energy consumption in atrium buildings [1–2, 11], it is important to have properly validated energy prediction methods to assist in the design of energy efficient atrium buildings.

The present work focuses on the accuracy of an energy

*Corresponding author. Tel.: 001 613 993 9629; fax: 001 613 954 3733; e-mail: morad.atif@nrc.ca

0360-1323/99/$—see front matter
PII: S0360-1323(98)00007-9

simulation computer program in predicting specific thermal parameters in an atrium. ESP-r [13] was considered in this study as the simulation tool. The specific objective is to compare predictions and field measurements related to thermal parameters in an atrium space.

2. Description of the case study

2.1. General description

The selected atrium is a three-storey building located in a suburban wooded site in the region of Ottawa (latitude 45.0 and longitude difference 0.7 east). The atrium has an octagonal shape with a pyramidal skylight and is surrounded by walkways that lead to adjacent meeting or interview rooms and office spaces. Adjacent spaces are not designed to receive daylight from the atrium. Figure 1 shows the plan and cross-section view of the atrium.

A linear corridor at each floor connects the atrium to a larger eight-storey atrium (the tower). The first floor houses the main building entrance, conference or meeting rooms and the reception desk, with a floor area of 380 m^2. The second and third floors are identical and are surrounded by offices and conference rooms, with a floor area of 108 m^2 each. The entire atrium has a volume of 2864 m^3. The principal access to the outside is through three doors, one is revolving, at ground level.

2.2. Fenestration

The skylight of the atrium is made of three different types of solar controlled glass units, labeled as type A, A1 and D1. Figure 2 shows a plan and cross-section view of the top fenestration and Table 1 summarizes the material on each layer of the glass unit. Each unit is triple-glazed, consisting of two air spaces and a low-emittance heat mirror sandwiched between an inner and outer layer of glass. The patterned glass has opaque horizontal ceramic frit lines applied across it. This pattern reduces the glazing area by 30% (70% open). This glazing system has calculated solar transmittance of 13%. The solar transmittance was calculated by averaging the solar transmittances of the glazing units based on an area-proportion-weighting factor. VISION-4 [14] was used to calculate the solar transmittance of each glazing unit. The calculated U-value of the skylight is 1.25 W/m^2C (without the frame).

The exterior glazed walls of the first floor are of type A with a solar transmittance of 22% and a U-value of 1.25 W/m^2C (without the frame).

2.3. Occupancy

The atrium space was occupied only during weekdays from 07:00–19:00 h, serving as a reception and a circulation space. Primary activities included standing and walking, with a minimum amount of reading or similar work occurring. Maximum occupancy occurred in the early morning (around 08:00 h) and in the late afternoon (around 17:00 h). The surrounding spaces were used for conferences and meetings.

2.4. Electrical lighting

The atrium employs a daylight controlled electrical lighting to provide acceptable level of illuminance inside the atrium space and to reduce electrical energy consumption. The electrical lighting fixtures are distributed as follows:

- 16 recessed incandescent fixtures (150PAR38) are placed along the perimeter of the ceiling of the walkway space for each floor. Eight are for the emergency lighting, and remain on continuously, while a daylight sensor located indoors in another atrium of the building controls the other eight fixtures.
- 10 continuously powered recessed incandescent task lighting fixtures (MR75) are placed above the reception counters of the first floor.
- 44 recessed incandescent fixtures (150PAR38) are placed in the ceiling of the open space surrounding the first floor (entrance, and corridors leading to the stairwells and the tower).
- 8 daylight-controlled recessed incandescent fixtures (500PAR56) are placed along the perimeter of the ceiling of the second floor and point towards the centre of the atrium floor at ground level.
- 8 manually controlled mercury vapour fixtures (MH175) are placed along the perimeter above the third floor and direct their light towards the atrium roof for twilight and nighttime lighting.

2.5. Mechanical system

The first floor is ventilated through four separate supply ducts: two of which supply the perimeter of the building through ceiling diffusers and two which supply the offices and the open space surrounding the atrium. The second and third floors of the atrium are ventilated through sets of 24 high velocity supply jets located on the edge of the ceiling. These jets have diagonal throws shooting downwards into the atrium core to prevent temperature stratification. The fenestration dome is not ventilated. On the second and third floors there are four ducts that supply the offices. All supply branches are provided with a mixing section, a filter section, a hot water heating coil, chilled water cooling coil and humidifier.

A variable air volume box controls the amount of air to be fed in a specific zone. A thermostat located in the ventilated space serves as a proportional-integral control-

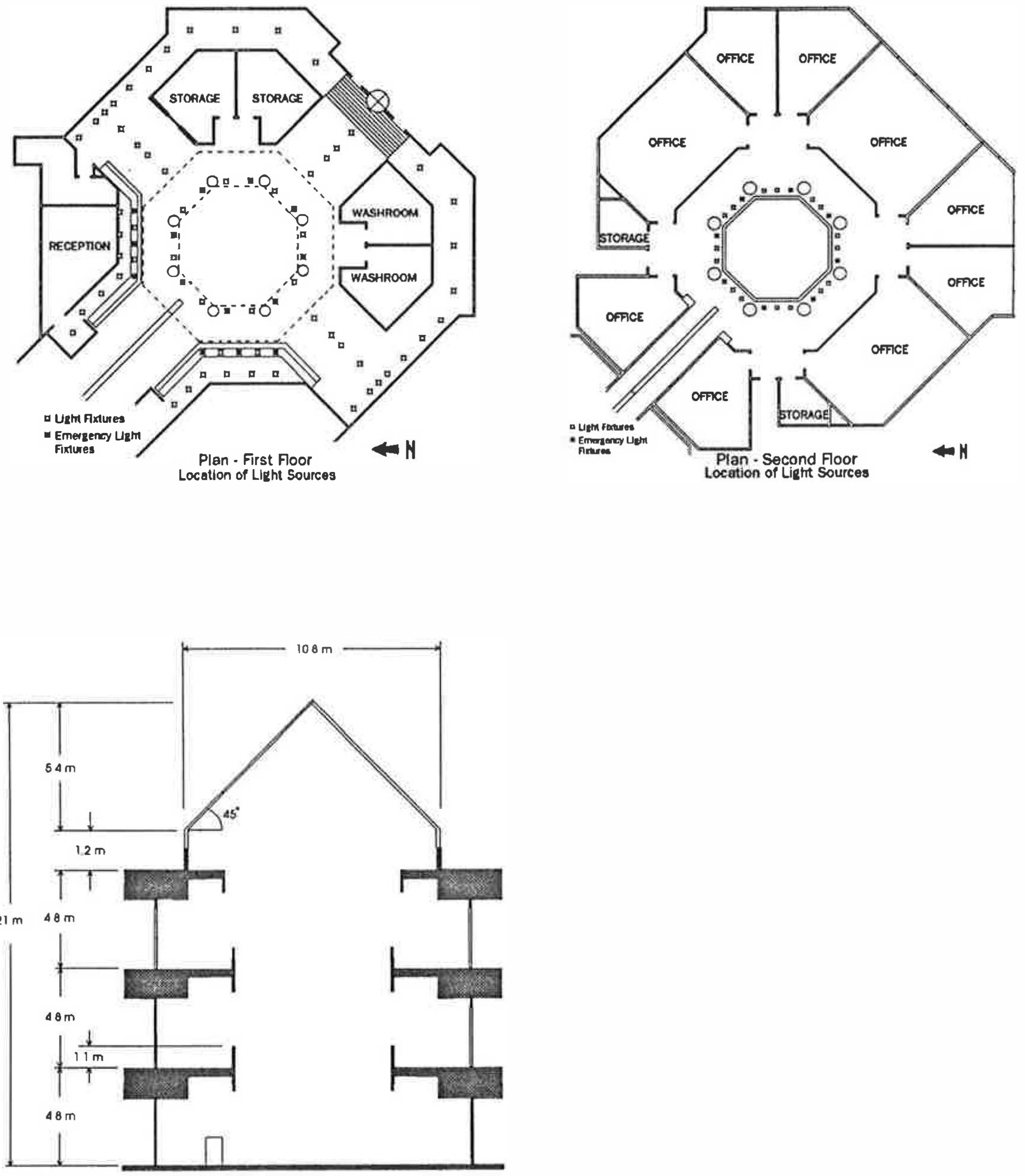

Fig. 1. Plan and cross-section view of the atrium.

ler. The four supply branches on the first floor and the jets on the second and third floors are all equipped with VAV boxes.

On the first floor, the return air is drawn through the ceiling tiles in the areas surrounding the atrium. On the second and third floors, there are four perforated ceiling panels for exhaust air. These panels are located in the small vestibules providing entry to the offices surrounding the atrium. The control of the return air flow through transfer blocks maintains a neutral pressure inside the atrium.

3. Field measurements

The field measurements were conducted in two phases. The first phase took place from 2–27 June 1995, to address summer conditions, and the second phase from 29 November–15 December 1995, to address winter conditions. Measured parameters included indoor temperatures in the atrium space and the adjoining spaces, outdoor temperature, outdoor solar radiation, indoor solar radiation below the fenestration (global horizontal), supply air flow rate and air infiltration rate. Time-of-use

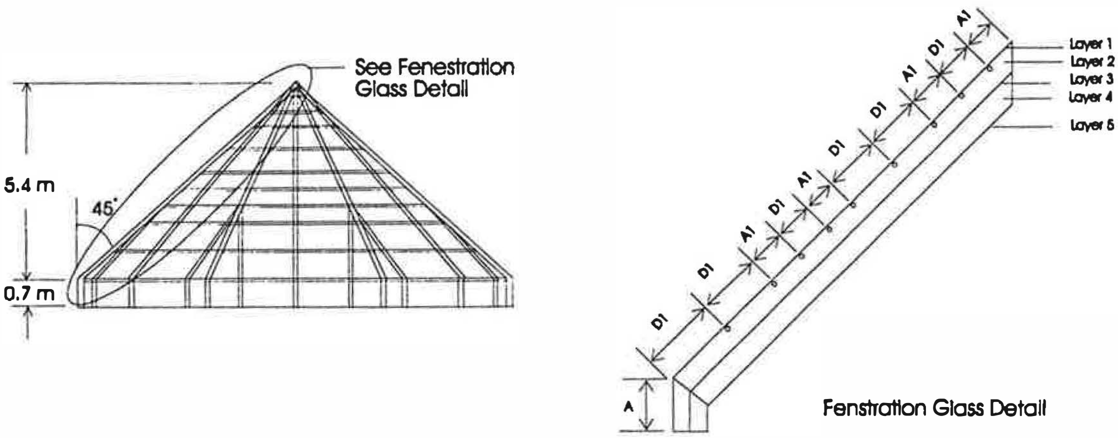

Fig. 2. Atrium fenestration.

Table 1
Skylight glass units

Glazing type	Layer 1 (exterior)	Layer 2	Layer 3	Layer 4	Layer 5 (interior)
A Low reflectance	6 mm heat strengthened clear glass	13 mm air space	HM66 clear polyester film	13 mm air space	6 mm clear glass
A1 Low reflectance	6 mm heat strengthened clear glass	13 mm air space	HM66 clear polyester film	13 mm air space	6 mm thick clear laminated glass
D1 Low transmittance	6 mm heat strengthened patterned green glass	13 mm air space	HM55 green polyester film	13 mm air space	6 mm thick clear laminated glass

of the electrical lighting fixtures in the atrium space was also measured using data loggers. In addition, separate tests were conducted in the summer and in the winter seasons to determine the contaminant migration pattern when released in the centre of the atrium at ground level, but the results of which are discussed in another report [15].

3.1. Temperature measurements

The atrium temperature was measured with three thermocouple trees dropping from an I-beam into the atrium core. The I-beam was set across the atrium dome from east to west. The thermocouple trees were 3.4 m apart. Each tree contained 11 thermocouples, which were 1.2 m apart. The highest thermocouple was at level of the I-beam itself at 14.4 m from the atrium floor. The lowest thermocouple was 2.4 m above the atrium floor. The temperature measurements were taken every minute and were stored as ten-minute averages. Each thermocouple was calibrated with a standard uncertainty of $\pm 0.1^{\circ}$C. Figure 3 shows the location of the thermocouples inside the atrium space.

In order to identify the impact of the mechanical system on temperature stratification, the mechanical system was turned off over the weekends of 10–11 June, 17–18 June, 2–3 December and 9–10 December. To stop air

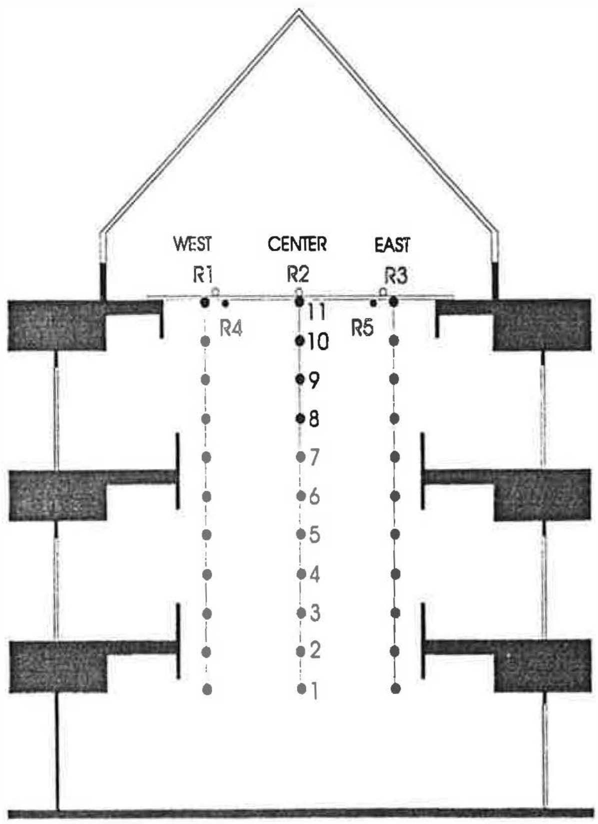

Fig. 3. Thermocouple and internal radiometer positions.

flowing into the atrium space from the rest of the building, panels were installed to block the corridors leading out of the atrium from 10:00 h on 2 December–17:00 h on 3 December. On 10 December, panels were installed temporarily from 10:00–17:00 h for the duration of the air infiltration measurement tests. Temperature and relative humidity were also measured in the adjacent spaces, but the results of the measurements are not shown in this study.

3.2. Solar radiation measurements

The outdoor and indoor (below the skylight) solar radiation was measured on-site. The outdoor solar radiation was measured at the rooftop weather station using radiometers. An automatically controlled shadow band periodically passed over the sensor in order to measure the diffuse horizontal radiation. When the band was removed from the sun, global horizontal measurements were taken. Direct normal radiation was automatically calculated from the diffuse and the global horizontal measurements. The complete measurement cycle took 15 s and 10-minute averages were recorded. Backup data with Epply device were also taken for reference. A maximum relative error of 13% was reported between the radiometer and the Epply device readings.

To measure net solar radiation entering the atrium space, three radiometers were installed below the west, centre and east side of the skylight to measure the transmitted solar radiation. Two other radiometers, facing downwards, were installed at the same apparatus to measure the outgoing solar radiation (see Fig. 3). The five radiometers were installed inside the atrium dome on an I-beam. The radiometers measured the global horizontal radiation.

The outdoor temperature was measured on-site, using shielded thermocouples every minute and stored also as 10-minute and 30-minute averages. Other outdoor parameters were collected at a meteorological station 15 km away from the monitoring site. These parameters include outdoor temperature (for reference), relative humidity, wind speed and wind direction. The latter three parameters could not be measured at the site. However, both sites offer the same micro-climate.

3.3. Mechanical system

Averaging tubes and pressure transducers were installed in each supply duct to measure the velocities of the air injected into the atrium space. The measurements were taken manually three times a day. The measured air flow rate did not change significantly throughout the monitoring period. Therefore, the air flow rate was assumed constant for the energy calculations. The amount of the air injected into the whole atrium space was 2257l/s with a supply temperature of 21°C in June 1995, and 1760l/s with a supply temperature of 23°C in December 1995.

4. Comparison criteria

Measured thermal parameters were considered for comparison between measured and predicted data. These are the instantaneous solar radiation admitted into the atrium space and the indoor temperature of each floor.

Net measured solar radiation (transmitted–outgoing) was compared to the absorbed solar radiation by all interior surfaces of the atrium walls:

$$G_{net} = G_{in} - G_{out} = \sum_{surf} G_{surf} \tag{1}$$

where:

G_{in} = averaged transmitted solar radiation at the rooftop (measured);
G_{out} = averaged outgoing solar radiation at the rooftop (measured); and
G_{surf} = absorbed solar radiation by the wall interior surface (predicted).

The average measured temperatures of the atrium floors were compared with the predicted temperatures. The average measured temperatures of the three floors are:

$$T_{f1} = 1/3 \sum_{i=1}^{3} \{T_i^{east} + T_i^{centre} + T_i^{west}\}/3 \tag{2}$$

$$T_{f2} = 1/5 \sum_{i=3}^{7} \{T_i^{east} + T_i^{centre} + T_i^{west}\}/3 \tag{3}$$

$$T_{f3} = 1/5 \sum_{i=7}^{11} \{T_i^{east} + T_i^{centre} + T_i^{west}\}/3 \tag{4}$$

where T_i is the measured temperature at level i of the I-beam.

5. Simulation

The simulation results presented in this paper were obtained using the ESP-r computer program [13]. The simulation focus was primarily on the atrium space. The adjoining spaces were considered as adjacent spaces with constant uniform temperatures. The volume, the geometry, the total surface and the geometry aspect-ratio of the simulated atrium were preserved to accurately predict heat exchanges. Figure 4 shows the atrium building as simulated.

5.1. Assumptions

To predict temperature stratification inside the atrium space, the latter was split into four stacked thermal zones, i.e., three floors and a roof. These thermal zones are separated by fictitious surfaces, which have 100% solar transmittance and negligible infra-red emissivity and *U*-value. Heat flow through these fictitious surfaces was accurately calculated by knowing the air flow rate passing through them. This flow rate was calculated by defining a mass flow network for the atrium space that was solved in tandem with the temperatures. The following assumptions were considered in the simulation:

- Each thermal zone was represented by a uniform temperature.
- All interior adjoining spaces to the atrium space were held at a constant temperature, i.e., 21°C. This assumption was derived from the measurements of temperatures of the adjacent spaces.
- The air motion pattern in the atrium space followed that analyzed during the monitoring of contaminant migration.
- The tower, which communicates through corridors with the case study atrium, was at constant temperature (21°C) and pressure. The pressure was estimated to produce a flow pattern similar to that analyzed during the monitoring of contaminant migration.

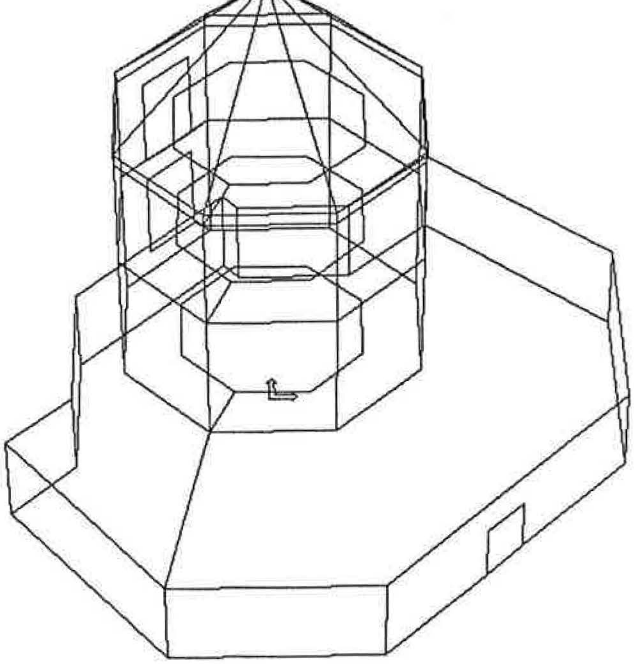

Fig. 4. The atrium as simulated.

- The exhaust system of the atrium was not considere in establishing the air flow balance of the atrium spac
- Since the air flow inside the atrium space was due t temperature and pressure differences, Cardiff's co relation for the interior convective heat transfe coefficient was used [13]. This correlation yields highe values of the convective heat transfer coefficient tha the ESP-r default Alamdari and Hammond correlatior
- Lighting energy in the second/third floors was assume to be apportioned, as half of it was picked up by th floor itself and the remaining half went to the immediat lower floor. This is because the lighting fixtures wer installed at the edge of the ceiling and pointed toward the first floor. In winter, all the daylight controlle fixtures and the open space lighting fixtures (entranc and corridors leading to the stairwells and the tower were on during the weekdays and weekends (99% tim of use). However, in summer, the measured schedule were used for the daylight controlled lighting. The ope space lighting fixtures were assumed to be off in th summer during the weekends. The convection part o the lighting energy for each floor, and the power facto of the lighting fixtures were assumed to be 0.2 and 1 respectively.

5.2. Air flow pattern and air leakage

The air flow pattern in the atrium space was simulated, based on tracer gas tests during the monitoring of contaminant migration, the results of which are reported in another report [15]. The leakage of the building was estimated as follows:

- Leakage through cracks between the exterior doors and their frames—a typical value of 2 mm/m of the crack width per crack length for weather-stripped standard doors (0.8 m × 2 m) was chosen [16]. The crack length in the exterior doors was about 20 m.
- Leakage through cracks in the glazed walls at the ground floor—a typical value of 0.25 mm/m was chosen with a crack length of 60 m.
- Leakage through cracks in the skylight—a value of 0.25 mm/m was selected with a crack length of 80 m.
- Leakage through cracks between interior doors and their frames in the adjoining offices of the second and third floors—only offices that have exterior walls were taken into account. A value of 2 mm/m was taken with a crack length of 25 m (for four standard doors).
- Leakage through open corridors—this was estimated as flow through large openings. The effective areas of the openings were chosen to yield approximately the same value of the measured air flow rate.

6. Results and discussion

The results are presented for the weekends only where the atrium space was not occupied, and the HVAC system was turned off.

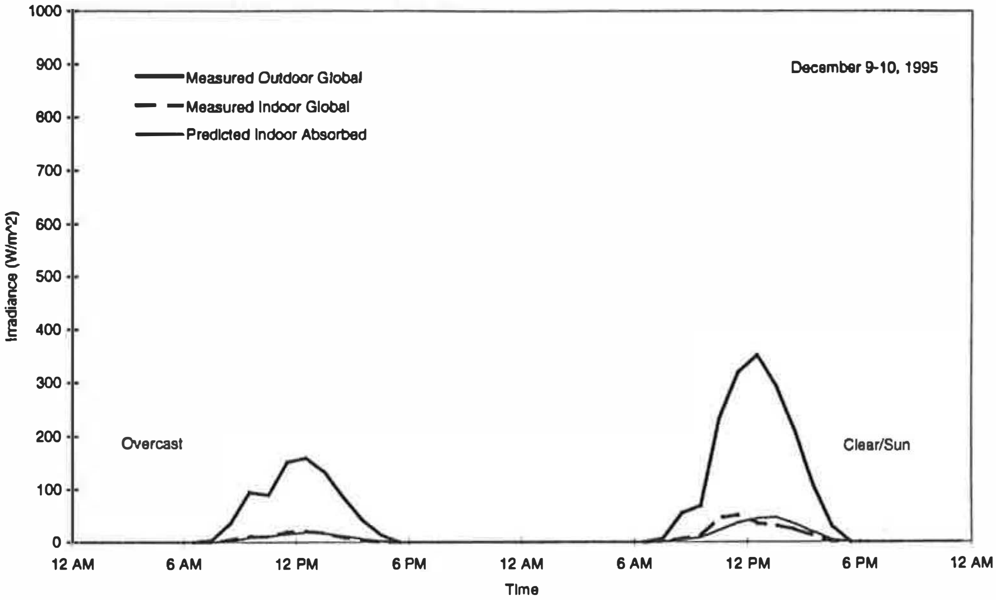

Fig. 5. Comparison between net measured indoor solar radiation and computed indoor absorbed solar radiation—winter.

Figures 5 and 6 show the predicted and measured hourly instantaneous solar radiation for 9–10 December 1995 and for 17–18 June 1995, respectively. The figures show the measured outdoor global horizontal solar radiation, the measured indoor global horizontal solar radiation just below the skylight, and the predicted absorbed solar radiation by interior surfaces of the atrium. The predicted and measured solar radiation below the skylight are expressed per unit of floor area. 9 December was an overcast day while 10 December was a clear sunny day. 17 and 18 June were partly cloudy days (intermittent sun).

The predicted and measured instantaneous solar radiation below the skylight followed the same trend. In winter, under overcast days, the net measured solar radiation below the skylight and the predicted absorbed solar radiation were almost identical. However, in summer under partly cloudy days, the predicted absorbed solar radiation was lower than the net measured solar radiation below the skylight. The maximum difference was about 20%.

Figures 7 and 8 show the measured and predicted indoor temperatures of the atrium floors on 2–3 December and 9–10 December, respectively. The HVAC system was turned off and the corridors were assumed open. The figures show that the measured temperatures

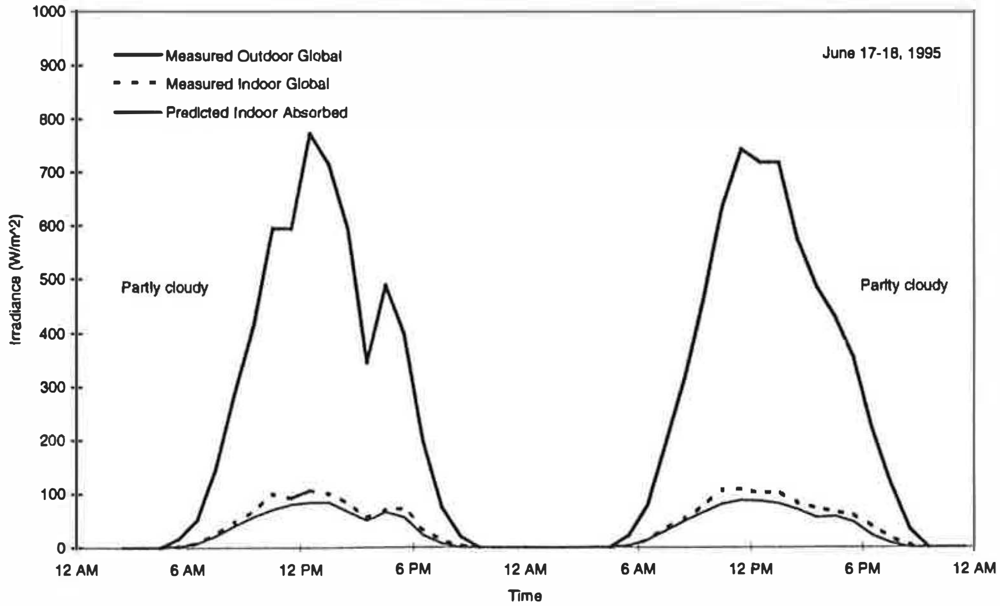

Fig. 6. Comparison between net measured indoor solar radiation and computed indoor absorbed solar radiation—summer.

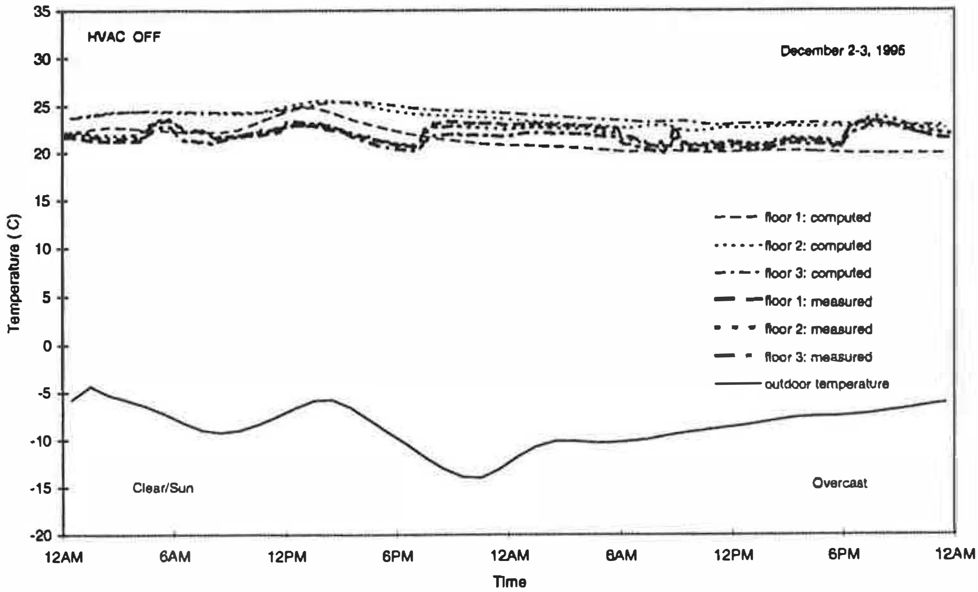

Fig. 7. Temperature of the atrium floors—2–3 December.

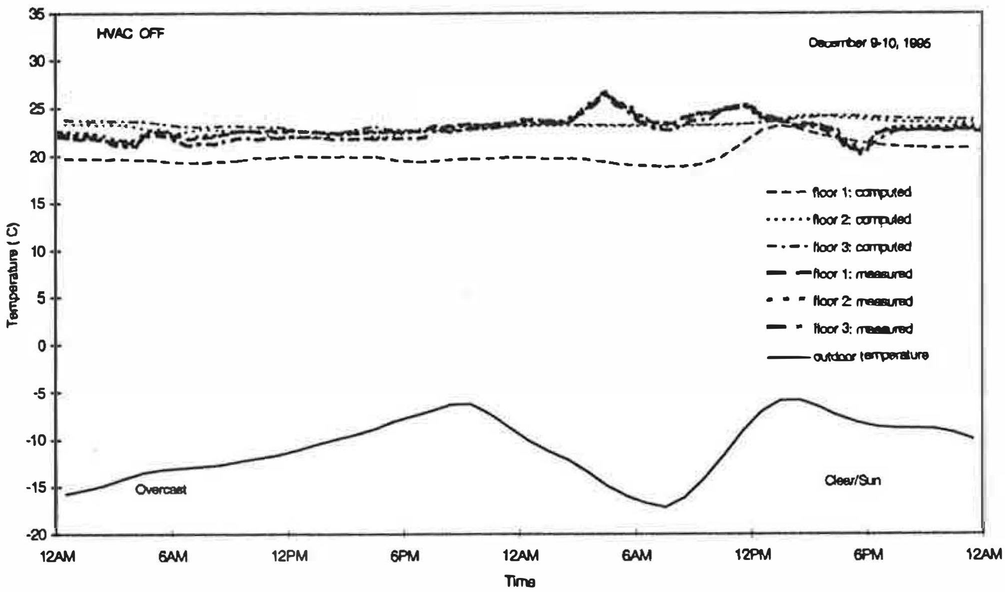

Fig. 8. Temperature of the atrium floors—9–10 December.

of the three floors were almost identical to the predicted temperatures of the second and third floors. The predicted temperature of the first floor was, however, lower by 2–4°C than the measured temperature. This difference was due to the fact that the temperature of the first floor was measured at the atrium core space, whereas the predicted temperature was the average of the temperatures of the atrium core space and the adjoining spaces (entrance space, corridors, meeting rooms) at ground level (which has interior and exterior walls).

Figure 9 shows the measured and predicted indoor temperatures of the atrium floors on 10–11 June. The HVAC system was turned off from 9 June at 07:00 h to 11 June at 17:00 h. Figure 9 shows that the temperature stratification as measured or predicted in the summer was pronounced, particularly in sunny days. The maximum predicted temperature of the atrium space was roughly the same as the maximum measured temperature (29°C). The predicted and measured temperatures of the atrium floors followed the same trend, and they were in reasonable agreement. The maximum difference between the measured and predicted temperatures was around 3 C. This difference between the measured and predicted temperatures may be due to the fact that one HVAC supply unit in the adjacent spaces of the first floor was not probably turned off completely.

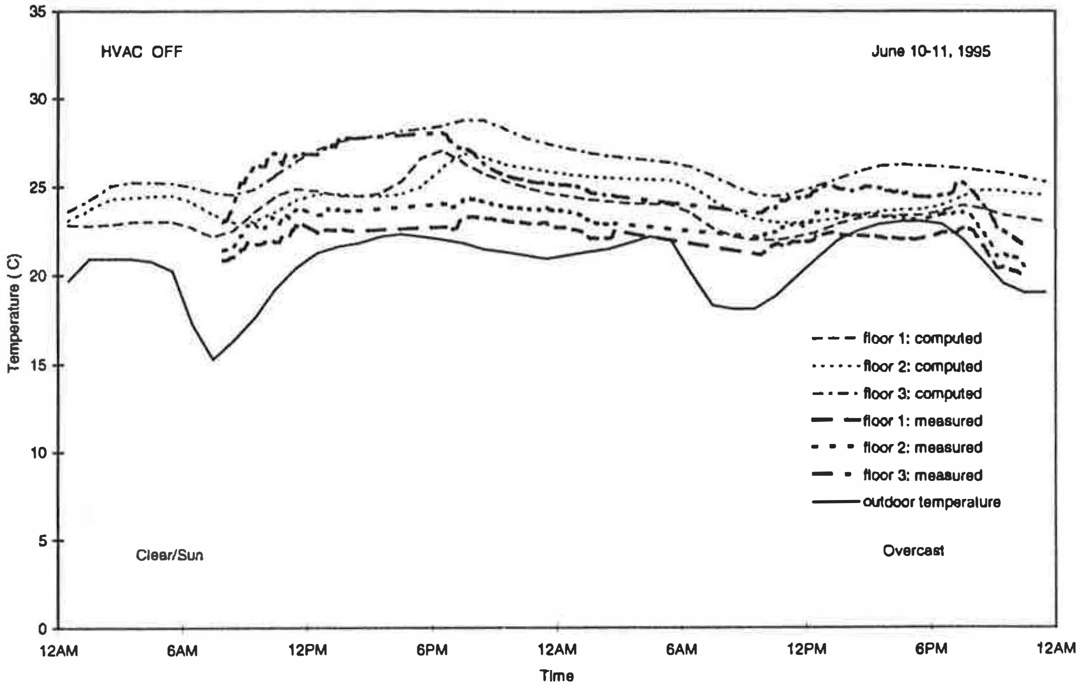

Fig. 9. Temperature of the atrium floors—10–11 June.

7. Conclusion

A comparison study between measured and simulated data has been made to test the capabilities of ESP-r in predicting the temperature stratification and in handling the solar radiation distribution passing through a complex glazing system to the atrium space. The atrium building was simulated during the weekends of June and December, 1995. The atrium space was not occupied and the mechanical system was turned off. The atrium floor temperatures were allowed to free-float according to the indoor and the outdoor climates.

The following points must be highlighted:

- The results for the solar radiation showed that in the winter, the predicted and measured solar radiations were in excellent agreement. However, in the summer under sunny days, the predicted solar radiation was lower by 20% than that measured.
- The results for the temperature in both winter and summer days showed a reasonable agreement between the measured and predicted indoor temperatures. In the winter, the predicted temperatures of the atrium floors were within $\pm 2^{\circ}C$ of the measured temperatures. In the summer, however, the predicted temperatures were 2–3°C higher than the measured temperatures. The maximum predicted temperature was approximately the same as the measured temperature (29°C).
- The measured and predicted temperatures in the atrium space showed that in the winter the temperature stratification was weak. However, in the summer, the temperature stratification was pronounced. The temperature stratification in the atrium space was mainly due to electrical lighting and solar radiation.

Acknowledgements

This work is part of a large project on atrium buildings, that was funded by the following organizations: Sociéte Immobilière du Québec; Public Works and Government Services Canada; Natural Resources Canada (CANMET); Hydro-Quebec; Institute for Research in Construction, National Research Council of Canada. Bell Northern Research Ltd. (Now Nortel Ltd.) provided access to their building. Robert MacDonald and Marcel Brouzes implemented the monitoring phase. James Reardon and John Shaw provided technical advice during the monitoring. Dr Joe Clarke and Jon Hand provided advice for the use of ESP-r.

References

[1] Atif MR, Claridge DE, Boyer LL, Degelman LO. Atrium Buildings: Thermal Performance and Climatic Factors. ASHRAE Trans., 1994. pp. 454–60.

[2] Wall M. Climate and energy use in glazed spaces. Report TABK-96/1009. Lund University. Lund Institute of Technology. Lund. Sweden. 1996.

[3] Hensen JLM, Hand L. Clarke JA. Building Design Assessment Through Coupled Heat and Air Flow Simulation: Two Case Studies. Proceedings of the Air Movement and Ventilation Control Within Buildings Conference. Ottawa. Canada. 1997. pp. 24–7.

[4] International Energy Agency, Annex 26. Energy-Efficient Ventilation of Large Enclosures. Ventilation of Large Spaces in Build-

ings, Part 3: Analysis and Predictions Techniques. In: Heiselberg P, Murakami S, Roulet CA, editor, 1997.
[5] Groleau D, Marenne C, Lefeuvre M. Simulation des écoulements D'air dans les espaces vitrés ensoleillés: Le cas d'une rue couverte. Proc of the European Conference on Energy Performance and Indoor Climate in Buildings. Tome 1, Lyon, France, 1994, pp. 161–6.
[6] Lomas KJ, Eppel H, Martin C, Bloomfield D. Empirical validation of thermal building simulation programs using test room data. IEA, 1994.
[7] Lomas KJ, Martin C, Eppel H, Watson M, Bloomfield D. 2, IEA, 1994.
[8] Lomas KJ. Empirical Validation of Thermal Building Simulation Programs Using Test Room Data. 3, IEA, 1994.
[9] Lomas KJ. Thermal Program Validation: The Current Status. Proceedings of the Building Environmental Performance Facing the Future, 1994. pp. 73–82.
[10] Saxon R. Atrium Buildings, Development and Design, 2nd Edition. London: Architectural Press, 1986.
[11] International Energy Agency. Passive Commerical and Institutional Buildings, Hastings SR, editor. Chichester, UK, John Willey and Sons, 1994.
[12] Hastings R. Myths in passive solar design. Solar Energy 1995;55(6):445–51.
[13] Energy System Research Unit, ESP-r, A Building Energy Simulation Environment. University of Strathclyde, Glasgow, UK, 1996.
[14] Advanced Glazing System Laboratory, VISION 4—Glazing System Thermal Analysis, Reference Manual. University of Waterloo, Ontario, Canada, 1995.
[15] Reardon JT, Atif MR. Monitoring Results of an Atrium Office Building: Part IV, Tracer Gas Measurements for Ventilation and Air Movement, NRC Internal Report, 1997.
[16] Clarke JA. Energy Simulation in Building Design. Adam Hilger Ltd, Bristol, UK, 1985.